COMBINING PHOTOGRAMMETRIC CAMERA AND IR VIDEOGRAPHY TO DEFINE WITHIN-FIELD SOIL SAMPLING FRAMEWORKS

Joanne Tapping, Keith B. Matthews, Gary G. Wright and Robert Wright[1]

Macaulay Land Use Research Institute
Craigiebuckler
Aberdeen, AB15 8QH
United Kingdom
Tel: +44 1224 318611
Fax: +44 1224 311566
Email: j.tapping@mluri.sari.ac.uk

[1] Department of Geography & Environment
University of Aberdeen
Elphinstone Road
Aberdeen, AB24 3UF
United Kingdom
Tel: +44 1224 272328
Fax: +44 1224 272331

ABSTRACT

This paper investigates the use of photogrammetric camera and IR videography data to improve the design of field survey sampling frameworks. Spatial data collection can contribute up to 80% of the cost of deploying a GIS (Geographic Information System) based land use decision support system. The use of remotely sensed information and geostatistical methods combined with field survey using dGPS (differential Global Positioning System) is expected to maximise data quality while minimising costs. The remotely sensed data used were medium format colour photography and IR (Infra-Red) videography. These were orthorectified to the national (Ordnance Survey) map base and mosaiced using ERDAS Imagine. ERDAS Imagine was also used to combine the blue, green and red layers of the colour photography with the IR videography into a single four layer image. The stratified sampling strategy adopted to date allocates four points per hectare randomly within individual field boundaries. The sample points, generated within ArcView, are located using dGPS. The data are then interpolated to a grid using geostatistics. A second strategy uses the remotely sensed information to identify within-field variability by means of classified soil or NDVI models. The sample sites are sub-stratified (at 4 per hectare) by variability classes with a minimum mapping unit of 0.25 hectare. Both strategies were employed at a test site and the results evaluated against validation samples collected on a 100m grid. The use of the remotely sensed information ensured that the survey sampled the range of within-field variability.

INTRODUCTION

Decision Support Systems (DSS) have been developed in response to increasingly complex financial, social and environmental goals of which land managers need to take account. Competition, regulation of land use, public awareness and changes in land ownership are factors identified as creating an increase in the demand for multi-objective land-use planning (Matthews *et al,* 1999). Critical in producing an effective, DSS for rural land use planning is the use of accurate data for characterising a site, such as its soils, which are collected from ground based surveys. However this can be costly, with the majority of the financial burden being carried by the client. It would therefore be beneficial to reduce the costs of data collection but still maintain the accuracy within the DSS. By using remotely sensed data it has been shown that the accuracy of the DSS could be improved (Moran *et al,* 1997) and/or the intensity of soil sampling frameworks could be reduced (Stein, 1998).

One problem in the use of a random, or grid based soil survey is the recognition of within-field variability. To account for such variability, studies have been conducted in which the sampling of soils is stratified using existing sources of information such as land use, soil maps units, a combination of both (Brus, 1994) and remotely sensed data. With respect to DSS, there is the additional problem of obtaining up-to-date information. Land use or soil maps may have been compiled many years previously and their accuracy may be questionable because the boundaries of various map units may have changed. These units may also not be a suitable basis for sampling the soil property of interest. Remotely sensed information offers the advantages of providing timely data collection and with the recent advances in sensor and image processing technology, with increasingly cost effectiveness.

The primary motivation behind choosing to combine medium format colour photography with IR videography is the flexibility it offers, particularly with regard to the timing of the capture and the scale of the

imagery, which are both important considerations. Although the costs of the purchase and processing of satellite imagery are reducing such that its use has become a more practical proposition for more people, there remains the difficulty of obtaining suitable images for Britain. In particular, weather conditions, especially cloud cover, limit the opportunity for capture of useable imagery. However, both the medium format metric camera and the IR video camera used in this paper, are deployed on a light aircraft which can be opportunistically tasked whenever conditions are acceptable. Aerial videography offers low-cost data acquisition with the flexibility of digital format, enabling the rapid processing of images, whilst conventional medium format colour aerial photography obtained using a calibrated lens can be accurately orthorectified with relative ease due to advances in software development.

The extraction of information from remotely sensed data is enhanced when it is combined with other data for the same area. The delimitation of units of within-field variability units, derived from soil and vegetation indices, can then be used to stratify sampling frameworks in a similar manner to the land use and soil maps used previously. The advantage of using the remotely sensed information is that it is up to date and not as subjective as land use and soil maps.

This paper proposes a methodology for designing soil sampling frameworks based on the integrated use of medium format colour photography and IR videography. The paper first presents the methodology adopted for the preparation and integration of the image data and then details the approach taken to structuring the soil sampling frameworks based on models of within-field variability. Two sampling strategies are then compared, one using variability classes identified with the remotely sensed imagery and the second using the field as the sampling unit. The effectiveness of the two sampling strategies is compared using the prediction accuracy of soil maps, geostatistically interpolated from the two sampling frameworks. Finally conclusions are drawn on the use of medium format colour aerial photography and IR videography for site characterisation within a DSS.

METHODOLOGY

The methodology used to combine photogrammetric camera imagery and IR videography to define within-field soil sampling frameworks is detailed in Figure 1.
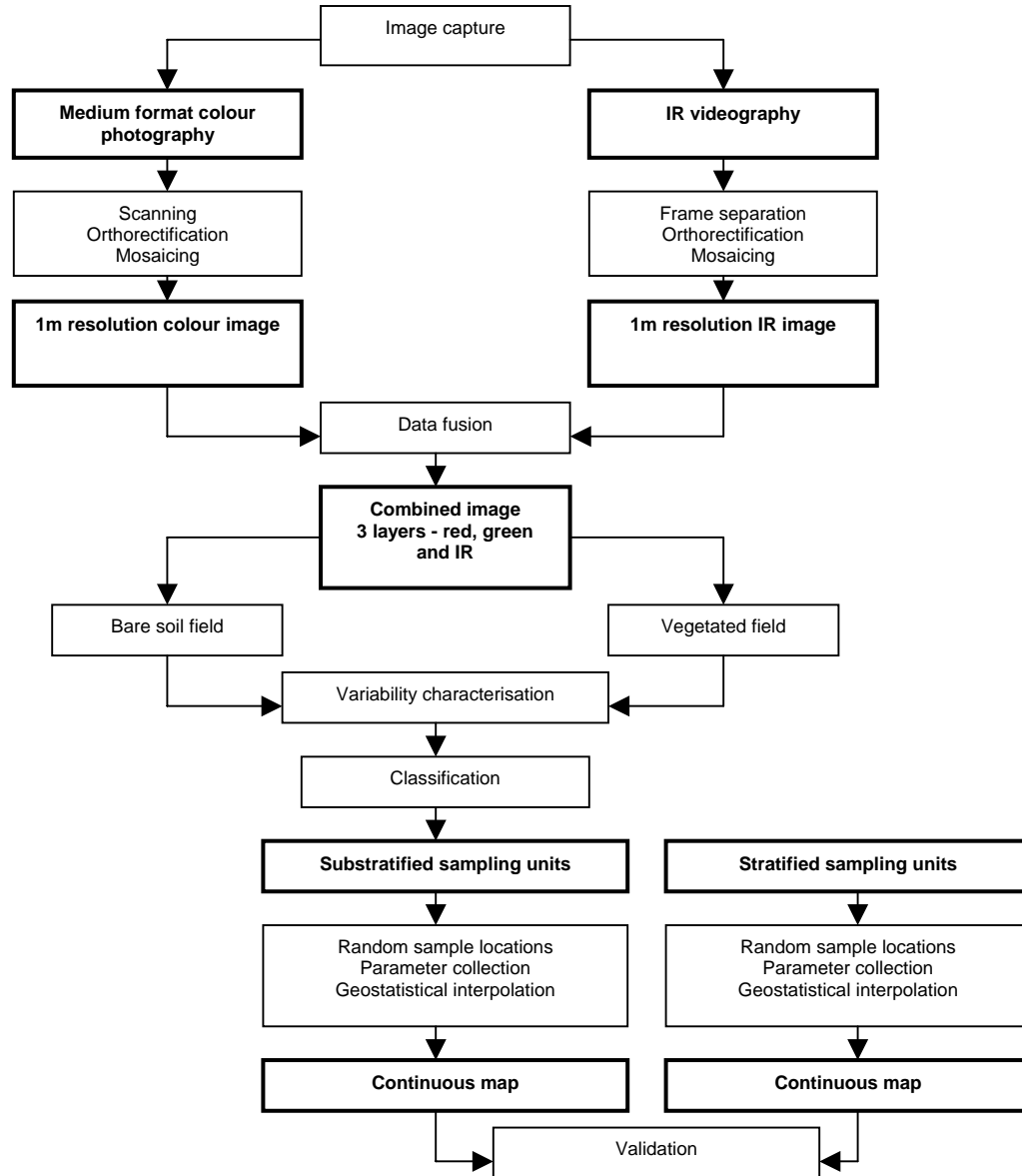
Figure 1. Outline of methodology employed

The flow chart details the sequence of procedures employed, from image capture through to the validation of the outputs from the two sampling strategies. The raw images are geometrically corrected (to an Ordnance Survey map base), mosaiced and then combined. Variability within bare soil and vegetated fields is highlighted and classified by processing the layers within the image. The variability is further defined within a GIS to produce 'variability units' within the field, which are then used to substratify the random samples. The substratified sampling framework is evaluated, for a given soil physical property, against a simple (by field) stratified framework and a set of validation samples, using geostatistical techniques.

Imagery Preparation

Medium Format Colour Aerial Photography. The colour aerial photography was obtained using a Rolleiflex 6006 metric camera with a Planar f2.8/80mm lens. The resulting 5 x 5" hardcopy prints (with a nominal ground scale of 1:5000) were flat-bed scanned at a resolution of 600 pixels per inch.

The colour photography was orthorectified using the ERDAS Imagine OrthoBASE software. The calibration information available for the camera, including interior orientation parameters, means that typically only 3 ground control points are required per image. A total of 20 ground control points were needed for the block of imagery and collected using digital map data. Terrain distortion was removed using a 5 m resolution Digital Elevation Model (DEM) derived in ESRI ArcInfo from 1:10,000 scale digital contour data. The colour photography was resampled to a resolution of 1 m using the nearest neighbour method. Figure 2 is an example of the orthorectified and mosaiced image from the test site detailed in the Testing section of the paper.

IR Videography. The IR videography was captured using a PULNiX TM765i (2/3 inch CCD array, with 756 x 581 pixels) video camera fitted with a Cosmicar f1.5/8.5mm lens and filtered using a Kodak Wratten 88a filter. The data was recorded on a Sony GV-S50E portable Video8 recorder. Individual frames with 60% overlap were manually selected and extracted using the SnapMagic framegrabber. Survey coverage was created by orthorectification, using ERDAS Imagine OrthoBASE and mosaicing using ERDAS Imagine. Figure 3 shows an example of the imagery derived from the IR videography for the test site used in this paper. The image was derived from six frames, resampled to 1m using a nearest neighbour interpolation algorithm.

Orthorectification of IR videography was greatly enhanced and simplified by ERDAS Imagine OrthoBASE software, which can compensate for the lack of camera calibration information associated with videography. Initial attempts at rectifying the IR videography imagery, however, pointed to the need for a significantly larger number of ground control points (45) compared with the metric medium format photography. Additional ground control points were collected using dGPS where insufficient could be obtained from mapped features. Terrain distortion was removed using the 5m resolution DEM. The errors associated with the exterior and interior orientation parameters in the triangulation results remained unacceptable despite the additional ground control. These were, however, subsequently greatly reduced when the lens manufacturer provided generic calibration data (particularly a more accurate estimate of focal length and radial distortion) and a full specification of the CCD array (enabling a precise specification of CCD pixel size). The final orthorectified images were overlaid with the map base data and visually inspected for any mismatch.

Image Mosaicing and Data Fusion. The images within the two datasets were mosaiced in ERDAS Imagine to create two continuous images. Prior to mosaicing the histograms of all images were matched to that of a central image, using a histogram match function in ERDAS Imagine. The red and green layers of the colour aerial photography were added to the single layer of the IR videography, to create a three layer image.

Figure 2. Orthorectified and mosaiced colour photography 1:5000

Figure 3. Orthorectified and mosaiced IR videography 1:5000

Deriving the Sampling Frameworks

The first application of the fused datasets was to characterise variability within two example vegetated and bare-soil fields and to use the information on the variability to guide the design of a soil sampling strategy.

Variability Characterisation –Vegetated and Bare Soils. The variability of the vegetated field was characterised using a *Normalised Difference Vegetation Index (NDVI)*. The fact that green vegetation has low reflectance at visible red wavelengths and high reflectance at near infrared wavelengths is the basis of a variety of vegetation indices. Variable look angle and illumination may affect a simple ratio index, i.e. the division of the near infrared band by the red band, the NDVI attempts to minimise these effects.

$$NDVI = (((Infrared - Red) / (Infrared + Red) + 0.05) \, 100)$$

The variability of the bare-soil field was characterised using a simple model of red band minus green band.

Classification. The NDVI and soil model images were processed to produce five classes in each dataset, by using an unsupervised classification. The unsupervised classification was used because of the lack of available ground truth data. Each field was classified separately to ensure that only the within-field variability was accounted for. Each classified image was then filtered using a 7 x 7 median filter.

Conversion to Polygons and Merging. The classified and filtered images were converted into polygon coverages to allow further analysis within a GIS environment. The default sampling density specified for the application was four points per hectare (10,000 m^2), the minimum sampling area was 2500 m^2. Consequently, no polygon with an area less than 2500 m^2 could be assigned a sample location since the area is below the minimum sampling area specified. All polygons with an area less than 2500 m^2 were merged with the largest nearest neighbouring polygon of the same class to ensure that all of the output polygons were greater than the minimum specified sampling area.

Sub-Stratified Sampling Framework. Sampling sites were randomly generated within each polygon, using a customised Avenue script in ArcView. It was specified that no points should be within two metres of another sample location, field boundary and variability polygon boundary. This was to take account of the accuracy of the dGPS (+/- 1m), which was used to locate the sample sites in the field.

TESTING

The effectiveness of the remote sensing based sub-stratification framework was compared with a simpler field based stratification strategy for a test site at Newton Rigg in NW England. For this study the imagery was captured in July 2000, at an altitude of 1737 m (5700 ft), with a nominal scale of 1:5000. Capturing the images at this time of the year reduced the effects of shadowing and the fields were also in a condition that allowed the analysis of both vegetated and bare soil fields. Both sampling strategies were employed for two fields within the study area, Ling Field, a bare soil field (at the time of imagery capture) and Cow Pasture, a vegetated field (at the time of imagery capture). A 100m grid based sampling strategy was used for validation purposes.

Parameters Collected

At each sample site, measurements of soil physical parameters were taken, including site drainage, topsoil depth, soil depth, topsoil texture, subsoil texture, percentage stones and soil drainage. The measurements were made in accordance with the Soil Survey of Scotland Handbook (MISR, 1984) standards. Each sample site was located using a dGPS (LR12 Omnistar 3000), attached to a handheld GIS (PocketGIS on a Newton Message Pad 2100).

Geostatistical Interpolation and Validation

To compare the two sampling strategies, predictions of the percentage stone content were produced for each field and for each strategy. Percentage stone content value was chosen. Each dataset was explored for spatial patterns by computing the omnidirectional variogram, directional variogram and anisotropy plots (Kaluzny *et al*, 1998). If a trend was present and identified it was removed. The variogram was then computed and modelled. Ordinary kriging was then performed using the variogram results. The output of the kriging process were maps of the predicted percentage stone content of the soils and associated error maps. Each prediction map was compared against the validation dataset, collected on a 100m grid basis.

RESULTS

Colour Photography and IR Videography Data Fusion

Cow Pasture.
Grass field.

Ling Field.
Bare soil.
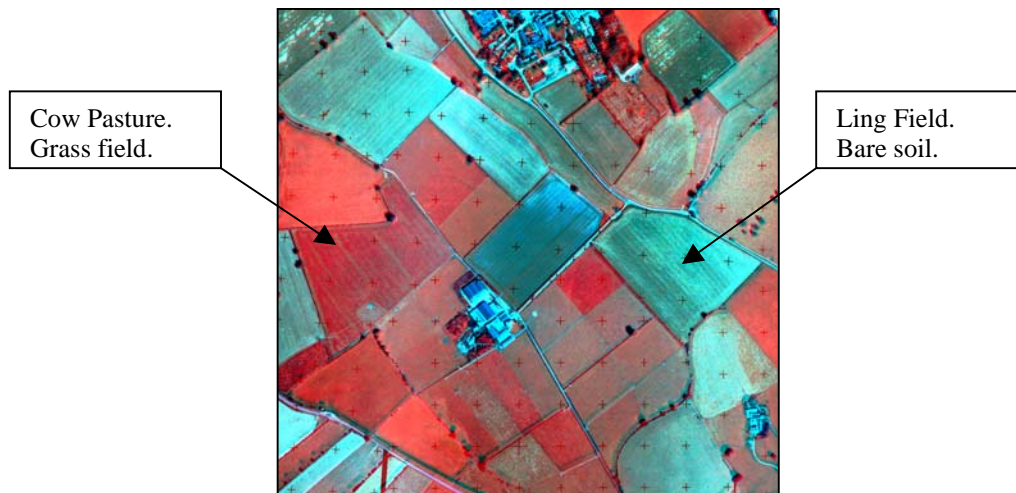
Figure 4. Red, green and IR combined image,
showing the fields studied.

By combining the red and green layers of the medium format colour photography with the single layer IR, as in Figure 4, variation can be seen within all the fields, including the two test fields, that is not visible in either the colour photography and/or the IR videography when viewed individually. Therefore, the within-field variability can be identified from the output of a combination of the different remotely sensed datasets output.

Soil and Vegetation Modelling. The next step in assessing the visible variation was to employ the soil and NDVI models, which took into account specific spectral properties of soil and vegetation.

a   b
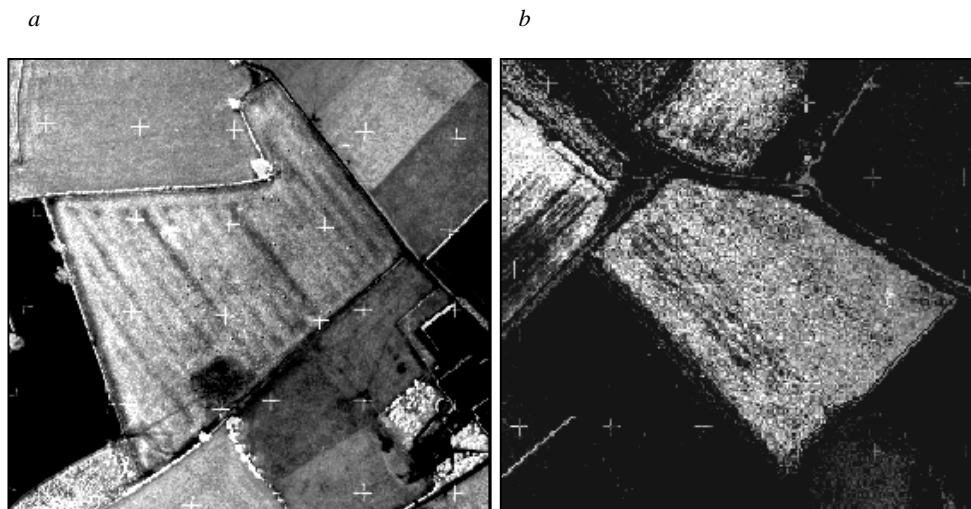
Figure 5. Output of the (a) vegetation model and (b) soil
model

Figure 5 (a) shows the output of the NDVI model. Contrast the very dark area to the west, a bare soil field with the central vegetated field. The level of brightness is indicative of the amount of biomass present, therefore the brighter a pixel the higher the biomass. Variation in biomass is clearly identifiable within the field.

Figure 5 (b) displays the output of the soil model. The central bare soil field is bounded to the south and east by vegetated fields, which show as the very dark areas. Patterns of variation are visible throughout the field. However, the variation seen is surface variation which may or may not be indicative of variation at depth. Soil variability classes arising from analysis of remotely sensed data may not correspond to soil map units derived from a traditional soil survey as traditional mapping units take into consideration properties at depths throughout the profile (Leone *et al*, 1995).

To further analyse the variation, the images were classified, using unsupervised classification. This had the effect of segmenting the images based upon the variation in the soil and NDVI model outputs.

a   *b*
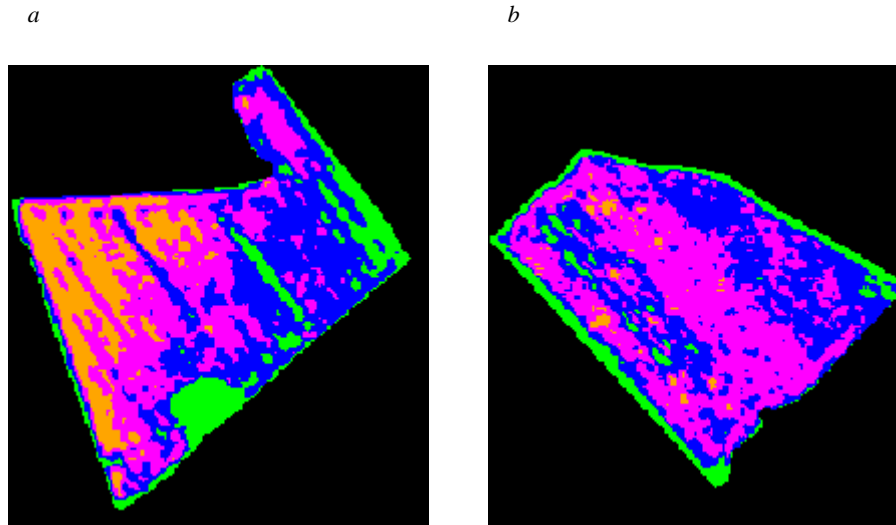
Figure 6. Classified and filtered outputs of the vegetation (a) and soil (b) models

Post-processing of the images, with a spatial filter, was used to clarify the differences in the variation (Figure 6).

Sampling Frameworks Comparison

a   b

Figure 7. The random and subrandom sampling frameworks within Cow Pasture (a) and Ling Field (b).

Figure 7 shows the subrandom locations based upon the variability polygons derived from the classified images and also the random sample locations based upon the field unit. As a result of classification, filtering and merging, Cow Pasture (Figure 7a) has been divided into five units and Ling Field (Figure 7b) into four units. By stratifying samples using these units, the sampling locations are spread across the field (compared to the simple random samples). The differences are particularly noticeable where the units are complex in shape, for example, the orange unit in Figure 7a. However, complexity of the variability units can also be the cause of problems. As it was specified that no sample location should be within one metre of another sample location, field boundary and variability polygon boundary, narrow (2m or less) polygons sections have been effectively eliminated from the sampling area, for example, the polygon along the outer edge of Ling Field (Figure 7b).

Geostatistical Interpolation and Validation

a   *b*
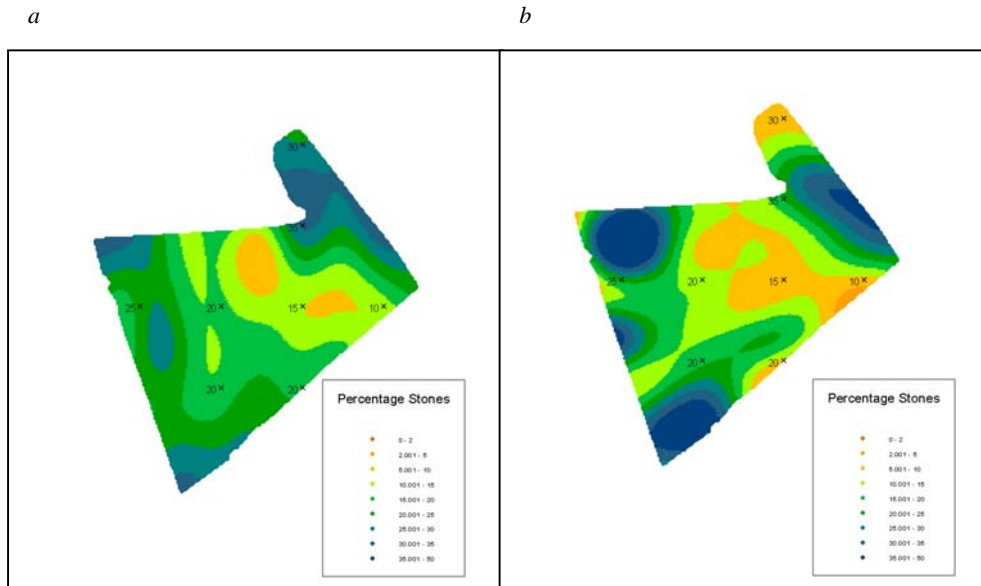
*Figure 8. Geostatistical interpolation of the subrandom (a) and random (b) datasets for Cow Pasture, overlain with the grid based validation (**X**) samples.*

Interpolation of the subrandom (Figure 8a and 9a) and random (Figure 8b and 9b) Cow Pasture datasets produce different maps of the distribution of percentage stones. When compared to the validation samples, seven out of the eight match the predicted surface generated from the subrandom dataset, whereas only three out of the eight match for the random dataset. The one validation point that did not match with the predictions had a percentage stone value of 10%, whereas the predicted surface assigned it a value of 15%. The differences between the values measured in the random dataset were quite different from those predicted, for example 30% compared to a predicted value of 10%. When compared back to the sample site locations (Figure 7a), this area is devoid of any random samples.
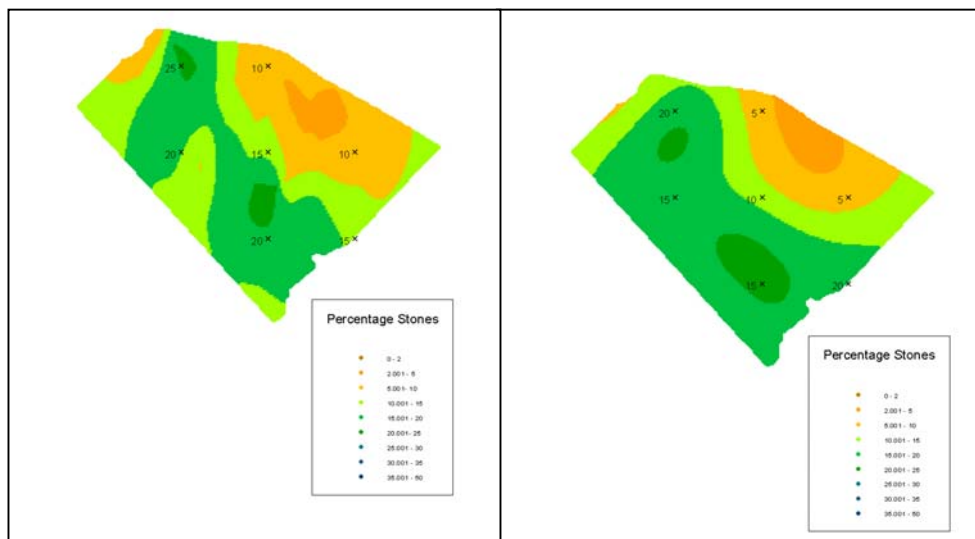
*Figure 9. Geostatistical interpolation of the subrandom (a) and random (b) Ling Field datasets, overlain with the grid based validation (**X**) samples.*

For the Ling Field subrandom dataset, all of the validation points matched with the predicted values. However, for the random dataset, four out of the seven validation points matched with the predicted values. Differences between the actual values and predicted values were not as striking as the differences experienced in Cow Pasture.

The errors associated with the kriging predictions are shown in Figures 10 and 11.
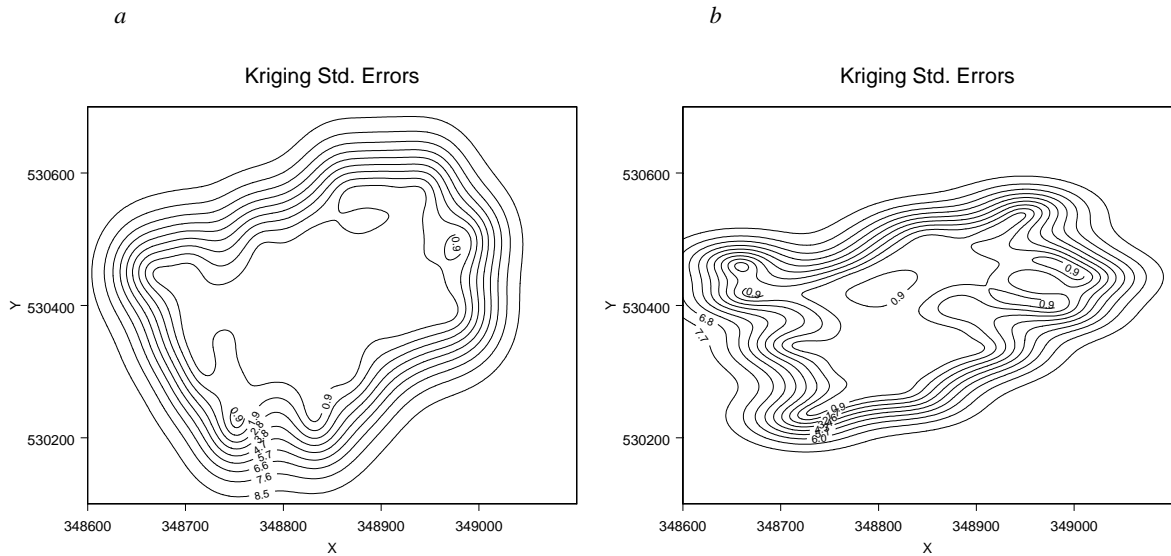
Figure 10. Cow Pasture kriging errors for (a) subrandom dataset and (b) random dataset

The prediction error contours for the Cow Pasture subrandom dataset range from 0.8 to 7.7 and for the random dataset from 0.9 to 7.7. Although both sets of data show the same range of error, the spatial distribution varies. The majority of the field is encompassed by the 0.8 contour in the subrandom prediction.
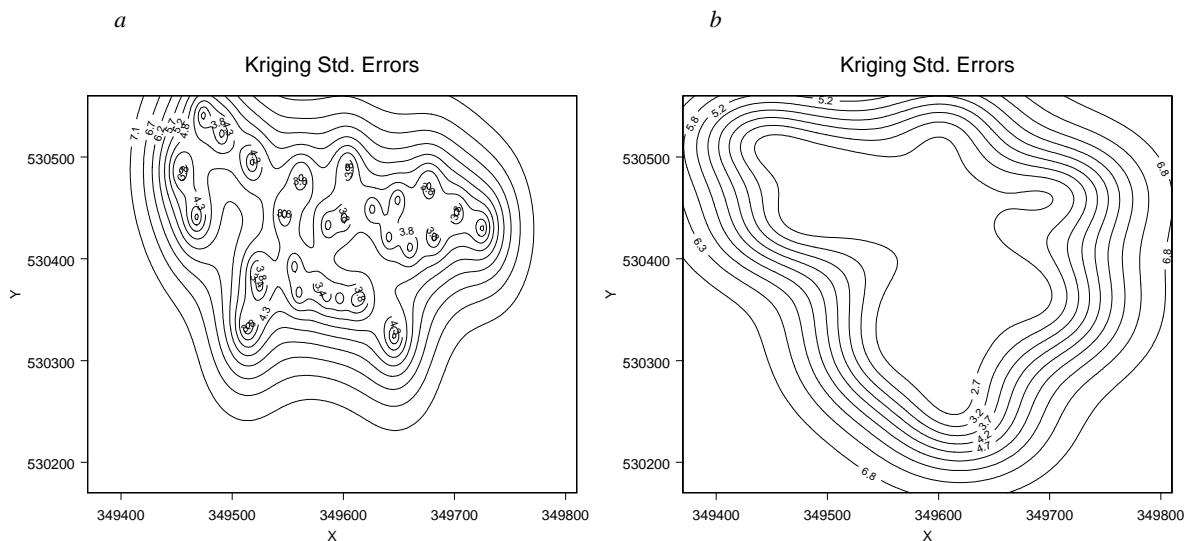
Figure 11. Ling Field kriging errors for (a) subrandom dataset and (b) random dataset

The prediction error contour for the Ling Field subrandom and random datasets range from 3.8 to 7.1 and 2.7 to 6.8 respectively. The subrandom dataset shows a higher degree of uncertainty associated with the predictions compared to the random dataset. The complex prediction contours for the subrandom dataset indicate that more of the variation within the field is sampled by the subrandom dataset. The uncertainty may also be accounted for by the fact that the variation observed in the remotely sensed data may not be correlated to the variation in the property under investigation. Accuracy of prediction may be enhanced by subsequently stratifying the interpolation using the derived variability units. Studies have shown that by using additional information during the interpolation process, prediction accuracy can be improved (Bárdossy and Lehmann, 1998).

CONCLUSIONS

This paper has presented the use of medium format metric aerial photography and IR videography to define sampling frameworks for soil survey. The aim was to reduce the cost or increase the accuracy of the mapping of soil properties to be used by land-use DSS. The colour aerial photography and IR videography images were orthorectified to a common map base and mosaiced to give survey coverage. Within-field variability was characterised using either vegetation or soil models. The classification of the outputs of these models provided the within-field stratification for the soil survey.

The use of light-aircraft mounted sensors enables four-band (R,G,B and IR) imagery to be captured at a low cost, reliably and at an appropriate scale. Difficulties in creating survey coverage from video images have been reported but advances in image processing software means that the problems of image mosaicing can now be overcome. The use of generic lens calibration data and engineering specifications for the video's CCD array are particularly helpful in this regard. The successful orthorectification of the video imagery does however require significantly greater level of ground control. The semi-automated process of ground control point acquisition means that this increased requirement for ground control can be met without making excessive labour demands. Additional ground control (particularly for elevation) may be collected using dGPS, again at relatively low (and decreasing) cost.

Combing the red and green layers of the medium format colour photography with the single layer of the IR videography produced an image from which within-field variation could be analysed using soil and vegetation (NDVI) models. More information could be extracted from the combined image due to the reflectance properties of bare soil and vegetation.

Stratification of the soil sampling frameworks by the derived within-field variability ensured that more features and smaller scale features were sampled. This subsequently resulted in soil property maps which accounted for more of the variation within the field and were more accurate when validated against grid based samples. Finally, the use of the remotely sensed information ensured that the field survey sampled the complete range of within-field variability.

REFERENCES

Bárdossy, A. and Lehmann, W. (1998). Spatial distribution of soil moisture in a small catchment. Part 1: geostatistical analysis. *Journal of Hydrology,* 206:1-15.

Brus, D.J. (1994). Improving design-based estimation of spatial means by soil map stratification. A case study of phosphate saturation. *Geoderma,* 62:233-246.

Kaluzny, S.P., Vega, S.C., Cardoso, T.P. and Shelly, A.A. (1998). S+ Spatial Stats: user's manual for Windows® and Unix®. MathSoft, Inc., Seattle, USA.

Leone, A.P., Wright, G.G. and Corves, C. (1995). The application of satellite remote sensing for soil studies in upland areas of Southern Italy. *International Journal of Remote Sensing,* 16(6):1087-1105

Matthews, K.B., Sibbald, A.R. and Craw, S. (1999). Implementation of a spatial decision support system for rural land use planning: integrating GIS and environmental models with search and optimisation algorithms. *Computers and Electronics in Agriculture,* 23:9-26.

Moran, M.S., Inoue, Y. and Barnes, E.M. (1997). Opportunities and limitations for image-based remote sensing in precision crop management. *Remote Sensing of the Environment,* 61:319-346.

Soil Survey of Scotland. (1984). *Organisation and Methods of the 1:250,000 Soil Survey of Scotland.* Macaulay Institute for Soil Research, Aberdeen.

Stein, A. (1994). The use of prior information in spatial statistics. *Geoderma,* 62:199-216.

Stein, A., Bastiaanssen, W.G.M., De Bruin, S., Cracknell, A.P., Curran, P.J., Fabbri, A.G., Gorte, B.G.H., Van Groenigen, J.W., Van Der Meer, F.D. and Saldaña, A. (1998). Integrating spatial statistics and remote sensing. *International Journal of Remote Sensing,* 19(9):1793-1814.

Wright, G.G., Matthews, K.B., Tapping, J. and Milne, R. (in preparation). "DIY Remote Sensing": Medium format colour photography and IR CCD shutter camera system for rapid site evaluation.